Iran J Sci Technol Trans Sci
https://doi.org/10.1007/s40995-018-0486-z

RESEARCH PAPER

Synthesis, Magneto-structural Properties and Colloidal Stability Studies of $Ni_{0.3}Zn_{0.7}Fe_2O_4$ Nanoparticles Coated with Pluronic P123 Block Copolymer for Potential Biomedical Applications

Cyril O. Ehi-Eromosele[1] · Benedict I. Ita[1,2] · Emeka E. J. Iweala[3]

Received: 19 November 2015 / Accepted: 16 March 2016

Abstract
Spinel $Ni_{0.3}Zn_{0.7}Fe_2O_4$ (NZFO) magnetic nanoparticles was prepared by the low temperature auto-combustion method using a glycine fuel-rich composition without any further heat treatment at high temperature. Subsequently, the synthesized MNPs were coated with Pluronic P123 (PP123) after its surface was functionalized with oleic acid (OA). The effect of the coatings on the morphology, structural and magnetic properties of NZFO nanoparticles was studied using powder X-ray diffraction (XRD), Fourier transform infrared, thermogravimetric analysis, field emission scanning electron microscopy (FE-SEM) and vibrating sample magnetometer (VSM). The colloidal behaviour of coated MNPs in physiological saline medium like water or phosphate buffer saline (PBS) was also studied by zeta potential measurements. XRD results showed the formation of cubic spinel crystalline phase with and without OA–PP123 coatings. Also, after OA–PP123 coating, the crystallite size (from Scherrer formula) decreases from 55 to 53 nm. However, an enlargement in the particle size and a reduction in agglomeration were observed from FE-SEM results when the nanoparticles were coated with OA–PP123. VSM measurements showed ferromagnetic behaviour at room temperature before and after coating. The colloidal stability study of the coated sample revealed a considerable high zeta potential value at physiological pH (7.4) highlighting its potential biomedical applications.

Keywords Magnetic nanoparticles · Coating · Biomedical application · Colloidal stability · PP123

1 Introduction

The biomedical applications of magnetic nanoparticles (MNPs) mostly in hyperthermia and targeted drug delivery have been extensively studied in the last two decades. Among nanomaterials used in biomedical applications, MNPs are particularly attractive because they have inherent magnetic properties. Thus, they can be remotely manipulated by an external magnetic field thereby serving as vectors for drug targeting (Banerjee and Chen 2007; Rahimi et al. 2010) or local heat sources in hyperthermia-based therapy (Jordan et al. 1999; Baldi et al. 2009). Furthermore, MNPs can be designed to combine therapeutic (hyperthermia and drug delivery) modalities to generate a synergistic effect for cancer treatment—the so-called multifunctional nanoparticles (Kulshrestha et al. 2012; Shah et al. 2012).

The spinel ferrites—ferro(i)magnetic or superparamagnetic nanomaterials, with general formula MFe_2O_4 (M = Mn, Fe, Ni, Co, Zn, Mg) which are stable and have appreciable magnetizations have been well investigated in biomedical applications. In this regard, superparamagnetic iron oxide nanoparticles (SPIONs) have been the most appealing because of their biocompatibility, low toxicity, ease of synthesis, enhanced specific loss power and easy functionalisation. However, there has been no consensus on the choice of the type of MNPs most suitable for biomedical applications as many studies (Kashevsky et al.

✉ Cyril O. Ehi-Eromosele
cyril.ehi-eromosele@covenantuniversity.edu.ng

[1] Department of Chemistry, Covenant University, PMB 1023, Ota, Nigeria

[2] Department of Pure and Applied Chemistry, University of Calabar, Calabar, Nigeria

[3] Department of Biological Sciences, Covenant University, PMB 1023, Ota, Nigeria

Published online: 24 January 2018

2015; Uskokovic et al. 2006; Maier-Hauff et al. 2011; Sakellari et al. 2016) have revealed the advantages of employing ferro(i)magnetic materials over superparamagnetic materials. Also, in spite of the numerous advantages of SPIONs, it is not possible to control the temperature distribution hence MNPs with tunable Curie temperature (T_c) are intensively investigated. Syntheses of several materials such as $La_{1-x}Sr_xMnO_3$ and $M_{1-x}Zn_xFe_2O_4$ (with M = Ni, Cu, Co, Mn) with adjustable T_c have been reported (Kuznetsov et al. 2002; Apostolov et al. 2013; Nguyen and Kyo-Seon 2014). $NiFe_2O_4$ is one of the most important spinel magnetic ceramics which finds interests in biomedical applications due to its low cost, excellent chemical stability, high electromagnetic performance and moderate saturation magnetization. Zn^{2+} ions, a non-magnetic substituent, have been used to reduce the T_c in spinel ferrites (Morrison et al. 2004; Gul et al. 2008). Among the series of $Ni_{1-x}Zn_xFe_2O_4$ compounds, the $Ni_{0.3}Zn_{0.7}Fe_2O_4$ (NZFO) has been calculated to have a T_c of $\sim$ 310–315 K which is suitable for biomedical applications like magnetic hyperthermia.

A major requirement for the biomedical applications of MNPs is the coating of their surfaces with a given biocompatible and functional layer. MNPs should be functionalized by organic or inorganic materials such as silica, polymers and other surfactants to achieve better physical and chemical properties. For example, this should lead to enhanced stable colloidal solutions and biocompatibility to prevent endocytosis by macrophages as well as to extend their residence time in blood circulation (Nguyen and Kyo-Seon 2014). The surface coatings can also provide functional surfaces for further modifications like in targeted drug delivery of anti-cancer chemotherapeutic agents. Mamani et al. (2013) has reported less agglomerated lauric acid-coated MNPs which can be used for biomedical applications. Dutz et al. (2007) showed that dextran coating of iron oxide nanoparticles not only influenced the magnetic behaviour of the nanoparticles but reduced significantly the agglomeration of the nanoparticles thereby making them very suitable for combined hyperthermia and chemotherapeutical applications. Dorniani et al. (2014) reported improvement in the thermal stability of both polyethylene glycol–gallic acid and polyvinyl alcohol–gallic acid coated SPIONs compared to their uncoated counterparts. Polyvinyl alcohol coatings on $Ni_{0.3}Zn_{0.7}Fe_2O_4$ nanoparticles were found to increase the relative sensibilities of the samples to the variation of applied frequency (enhancing their hyperthermia-based therapy applications) compared to the uncoated samples (Rahimi et al. 2013).

In the present study, an attempt has been made to prepare NZFO MNPs using a glycine-mediated low temperature combustion method and subsequently coated these nanoparticles with oleic acid (OA) and then stabilised with a block copolymer Pluronic P123 (PP123). Similar type of formulations has been extensively studied for iron oxide MNPs (Morales et al. 2005; Gonzales and Krishnan 2007) and lanthanum strontium manganite MNPs (Thorat et al. 2014) for biomedical applications. Since the coating of polymers on the surface of MNPs can alter some important properties of the particles, the effect of PP123–OA coatings on the structural, morphological and magnetic properties is discussed in detail. The colloidal stability of bare and PP123-coated NZFO MNPs in water was examined. The colloidal stability of PP123-coated NZFO MNPs in phosphate buffer solution (PBS) at pH 7.4 (physiological pH) and pH 5.0 (cancer cell endosomal pH) was also studied to highlight its stability in different physiological media.

2 Experimental

2.1 Materials

Nickel nitrate [$Ni(NO_3)_2{\cdot}6H_2O$], zinc nitrate [$Zn(NO_3)_2{\cdot}6H_2O$], and iron nitrate [$Fe(NO_3)_3{\cdot}9H_2O$] obtained from Sigma Aldrich, Germany are taken as oxidants while glycine ($C_2H_5NO_2$) obtained from SD Fine Chem. Ltd., Mumbai was employed as fuel to drive the combustion process. Triblock co-polymer PP123 (M.W. $\sim$ 5800) and oleic acid (OA) are Sigma-Aldrich, Germany products. All the reagents are of analytical grade and are used as-received without further purification.

2.2 Synthesis of NZFO MNPs

The spinel NZFO MNPs were prepared by the low temperature auto-combustion method using a glycine fuel-rich composition without any further heat treatment at high temperature. The advantage of combustion synthesis with glycine in a fuel-rich composition has been studied in our recent publication (Ehi-Eromosele et al. 2015). Stoichiometric amounts of $Ni(NO_3){\cdot}6H_2O$, $Zn(NO_3)_2{\cdot}6H_2O$, $Fe(NO_3)_3{\cdot}9H_2O$ and over-stoichiometric amounts of $C_2H_5NO_2$ were dissolved in 20 mL of de-ionised water. Then the solutions were heated to 80 °C to form a viscous gel of precursors under magnetic stirring. Second, the gel was transferred to a pre-heated coil (300 °C). Finally, after a short moment, the solution precursors boiled, swelled, evolved a large amount of gases and ignited, followed by the yielding of puffy black products. The powder (auto-combustion powder) was heated in a hot air oven at 200 °C for about 12 h to remove any organic product or unreacted glycine.

2.3 Synthesis of Surface-Coated NZFO MNPs

The synthesis of the surface-coated NZFO MNPs was carried out using the procedures reported by Thorat et al. (2014) but with slight modifications. First, to achieve the OA coating of NZFO MNPs, the NZFO MNPs (100 mg) were dispersed in methanol (100 mL) by sonication for 20 min. During the sonication, oleic acid (10 mL) was added into the solution. The solution was then heated at 75 °C with vigorous stirring for the complete removal of methanol by evaporation and then cooled to room temperature. The solution was washed three times with acetone and filtered. The filtered particles were redispersed in acetone to remove excess oleic acid and the final particles (NZFO–OA) were collected. In the second step, the coating of PP123 on OA-coated NZFO MNPs was done. 20% (corresponding to total weight of NZFO–OA MNPs) PP123 was dispersed in 100 mL distilled water at 60 °C with stirring. 100 mg NZFO–OA was added to the solution and ultrasonicated for 30 min for well dispersion of OA-coated MNPs. The solution was stirred in a closed container for 48 h. After stirring, the particles were separated by ultracentrifugation at 10,000 rpm for 20 min, with the supernatant discarded and the sediment washed with distilled water thrice and then dried at 60 °C for 1 h. The prepared sample (OA–PP123–NZFO MNPs) is used for further characterisations.

2.4 Physico-Chemical Characterisation

The X-ray diffractograms of the bare and coated (OA–PP123–NZFO) MNPs were recorded using an X-ray diffractometer (D8 Advance, Bruker, Germany), equipped with a Cu Kα radiation source ($\lambda = 1.5406$ Å) and the crystallite size was calculated by the well-known Debye–Scherrer relation:

$$D = \frac{0.9\lambda}{\beta \cos\theta} \tag{1}$$

where β is the full-width at half maxima (in radians) of the strongest intensity diffraction peak (311), λ is the wavelength of the radiation and θ is the angle of the strongest characteristic peak. Equation 2 was employed to calculate the lattice parameter (a) using the value of d-spacing of the strongest intensity diffraction peak.

$$a = d_{hkl}\sqrt{h^2 + k^2 + l^2} \tag{2}$$

where h, k and l are the Miller indices of the crystal planes and d_{hkl} is the separation of lattice planes. X-ray density (D_x) was calculated using the following equation:

$$D_X = \frac{8M}{Na^3} \tag{3}$$

where M is the molecular weight, N is the Avogadro's number, and a is the lattice constant. The surface morphology was examined with a Field Emission-Scanning Electron Microscopes, Nova Nano SEM 600 (FEI Co., Netherlands). Thermal decomposition behaviour of bare and OA–PP123–NZFO MNPs was carried out in a temperature range of 30–1000 °C in argon atmosphere with a heating rate of 10 °C/min using STA 409 PC Luxx from NETZSCH-Geratebau (Germany). The OA and PP123 coatings were investigated using Fourier Transform Infrared spectroscopy (ALPHA, Bruker) in the range of 400–4000 cm^{-1}. The magnetic characterisations were carried out with a Vibrating Scanning Magnetometer (Lake Shore cryotronics-7400 series) under the applied field of ± 20,000 G at room temperature. Zeta potential measurements were performed using a zeta sizer (Nano Zs, Nano series Malvern instruments). Measurements were taken in water and in PBS. Zeta potential measurements were done thrice for each sample at 30 electrode cycles.

3 Results and Discussion

3.1 OA–PP123 Coating of NZFO MNPs

PP123 were chosen for micellar encapsulation of NZFO MNPs due to its biocompatibility and safety. PP123 are approved by FDA for pharmaceutical and medical applications (Chiappetta and Sosnik 2007). PP123 is a water soluble tri-block copolymer composed of a hydrophobic central segment of poly (propylene oxide) [PPO] flanked by two hydrophilic segments of poly(ethylene oxide) [PEO]. Under the condition of over critical micelle concentration (CMC) in aqueous solution, amphiphilic block copolymers can spontaneously form micelles to reduce free energy which comes from hydrophobic interactions in aqueous solution or physiological environment (Song et al. 2009). The individual block copolymer molecule can be self-assembled into the micelles, and form core shell structure, where the MNPs are located in the core and thus can be effectively protected; have very low toxicity to human body, a prolonged circulation time in the blood owing to its evading scavenging ability by the macrophage system and renal clearance owing to its hydrophilic micelles shell (Song et al. 2009). First, the MNPs were coated with OA, acting as an adhesive to provide affinity to PP123 copolymer for its easy attachment to the MNP. As a surfactant, OA also helps to reduce particle agglomeration which may occur due to dipole–dipole interactions and hydrophobic nature of NZFO. Figure 1 shows a schematic representation of the coating of NZF sample with OA and PP123.

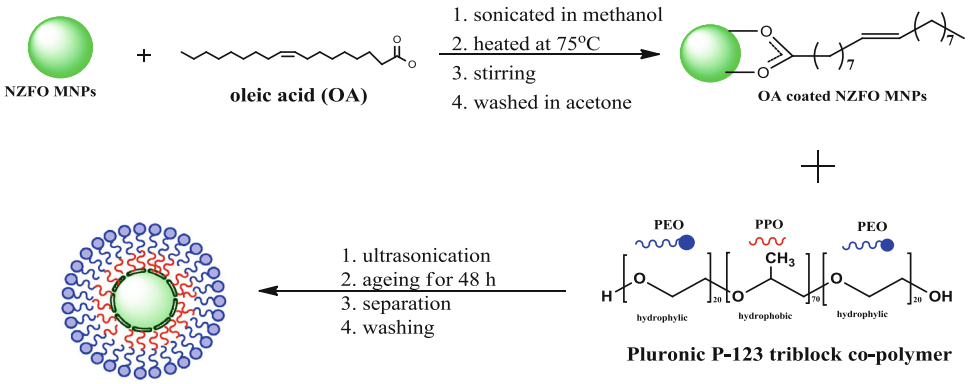

Fig. 1 Scheme shwing the coating of NZFO MNPs with OA and PP123

3.2 X-ray Diffraction

XRD was performed on the OA–PP123-coated NZFO MNPs and the pattern is shown in Fig. 2. The effects of OA–PP123 coating on the structural properties of NZFO MNPs are presented in Table 1. Like the XRD of the bare sample, the diffraction peaks have the characteristic peaks of spinel cubic structure (JCPDS card no. 10-0325). This clearly showed that the sample retained the spinel structure even after coating by OA–PP123 but with a suppression of diffraction peaks apparently due to the presence of OA–PP123 coatings which affects the surface of MNPs and induces internal strain due to lattice mismatch. There is a pronounced change in the calculated structural properties of the coated sample with the coated sample recording higher values of all calculated structural properties than the bare sample. The changes in the structural properties of coated sample might be due to the OA–PP123 coating. The calculated crystallite sizes (D) for bare and coated NZFO MNPs are 55 and 53 nm, respectively (Table 1).

3.3 FTIR Spectra

The FTIR spectra of bare, OA-coated and OA–PP123-coated NZFO MNPs are shown in Fig. 3. In case of the bare sample, the band observed at 536 cm^{-1} corresponds to stretching vibrations of Fe–O which is a typical metal–oxygen absorption band for the spinel structure of the ferrite. There is a shift of this absorption band to 537 cm^{-1} in the OA-coated sample and to 533 cm^{-1} in the OA–PP123-coated sample confirming the presence of the ferrite NPs in both nanocomposites. For the OA-coated sample (Fig. 3b), the weak peak at 1255 cm^{-1} is due to C–O stretching; and the peaks at 1453 and 1533 cm^{-1} are corresponding to the asymmetric and symmetric COO^{-} stretching modes, respectively. These two peaks are attributed to the oleate ion immobilised on the MNPs surface (Montagne et al. 2002). The band at 1709 cm^{-1} is due to the stretching vibration of C=O in OA. The absorption peaks at 2918 and 2851 cm^{-1} were attributed to the asymmetric CH_2 stretching and the symmetric CH_2

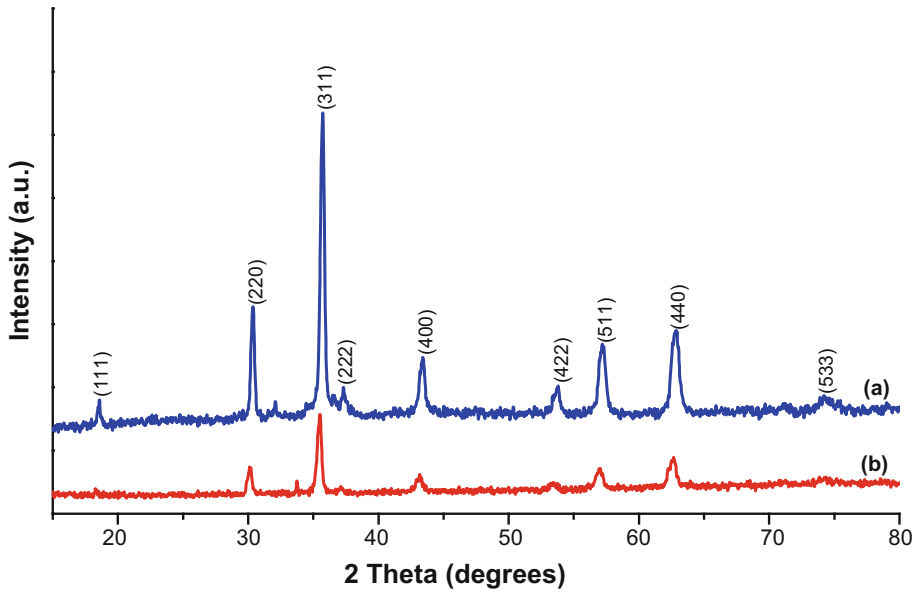

Fig. 2 X-ray diffraction patterns of a bare and b OA–PP123-coated NZFO MNPs

Table 1 Effects of OA–PP123 coating on the structural properties of NZFO MNPs

$Ni_{0.3}Zn_{0.7}Fe_2O_4$ MNPs	Crystallite size, D (nm)	Lattice constant, a (nm)	Unit cell volume, V ($nm^{3)}$	X-ray density, D_x (g/cm^3)
Uncoated	55	0.833	0.578	5.495
OA–PP123 coated	53	0.838	0.588	–

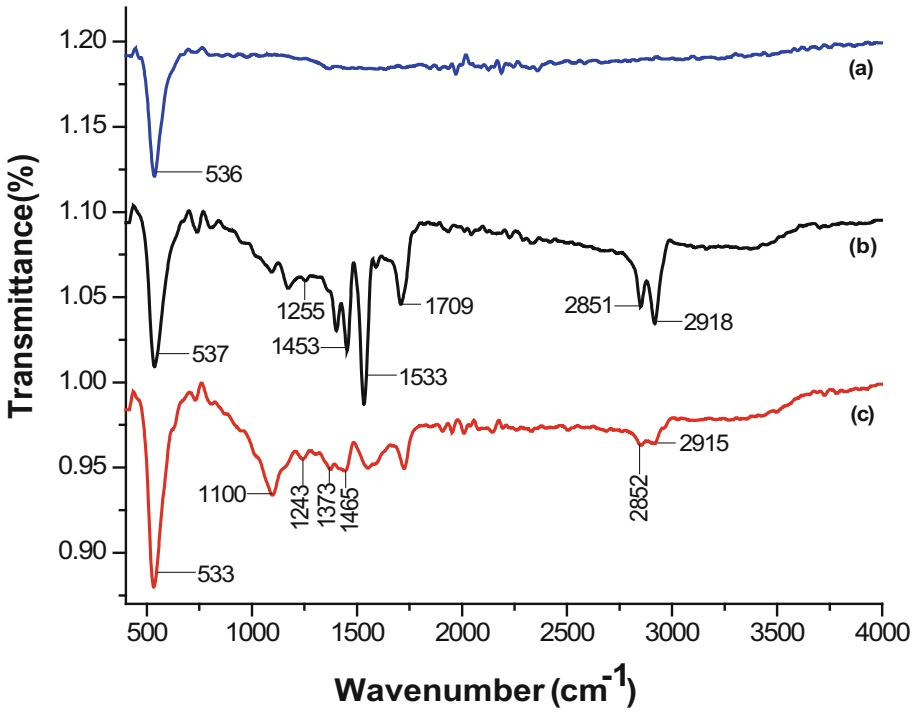

Fig. 3 FTIR spectra of NZFO MNPs. a Bare, b OA coated and c OA–PP123 coated

stretching, respectively. For the OA–PP123-coated sample (Fig. 3c), the peaks at 1100, 1243, 1373 and 1465 cm^{-1} correspond to the C–H stretching and deformation vibrations of PP123 polymer. The absorption peaks at 2915 and 2852 cm^{-1} were attributed to the asymmetric CH_2 stretching and the symmetric CH_2 stretching, respectively, as present in PEO. The result of the significant shift of the ferrite peak in the OA–PP123-coated sample to a lower frequency indicated that the hydrocarbon chains in the monolayer surrounding the nanoparticles were in a closed packed crystalline state (Mahdavi et al. 2013). The FTIR study confirms the attachment of OA–PP123 coatings on the NZFO MNPs.

3.4 Morphological Analysis

The morphology of bare and OA–PP123 NZFO MNPs was determined by FE-SEM. Figure 4 shows typical FE-SEM images of bare and OA–PP123-coated NZFO MNPs. It can be seen from Fig. 4 that there is an enlargement of NZFO particles after OA–PP123 coating thereby negating the results obtained from XRD. It is important to state that the crystallite size is determined on the basis of XRD pattern of nanoparticles whereas the particle size determined is the overall size of the composite. Usually, the particle size calculated from FE-SEM/TEM is higher than that of crystallite size calculated from the XRD (Jadhav et al. 2015). Also, in the presence of a polymer, small particles have tendency to join together and constitute large particles. Similar results have also been reported for polyaniline/$NiFe_2O_4$ (Khairy 2014) and PEG/$Mn_{1-x}Zn_xFe_2O_4$ (Kareem et al. 2015) nanocomposite systems. The bare sample displays an irregular and agglomerated morphology while the coated sample shows a more regular shape and lesser agglomeration. Lesser agglomeration after coating may be attributed to the presence of the non-magnetic surface layer of OA–PP123 which readily decreases the interparticle interaction of the MNPs.

3.5 Thermogravimetric Analysis

TG analysis of bare and OA–PP123-coated NZFO MNPs is shown in Fig. 5. TGA for bare NZFO MNPs (Fig. 5a) shows a little gain in weight (about 2%) which might be

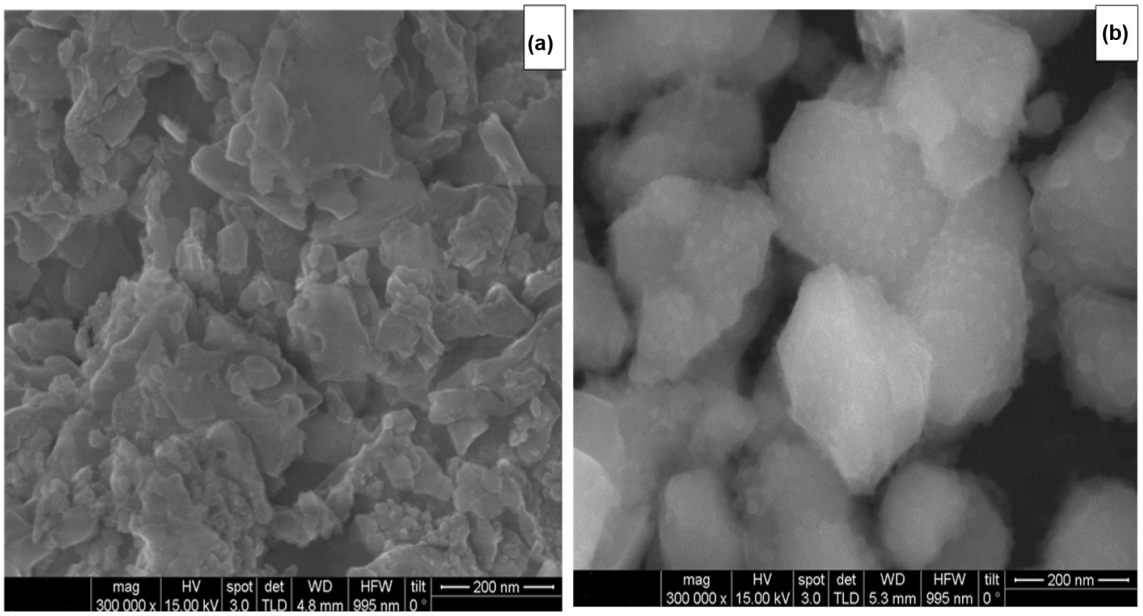

Fig. 4 FE-SEM images of NZFO MNPs. a Bare and b OA–PP123 coated

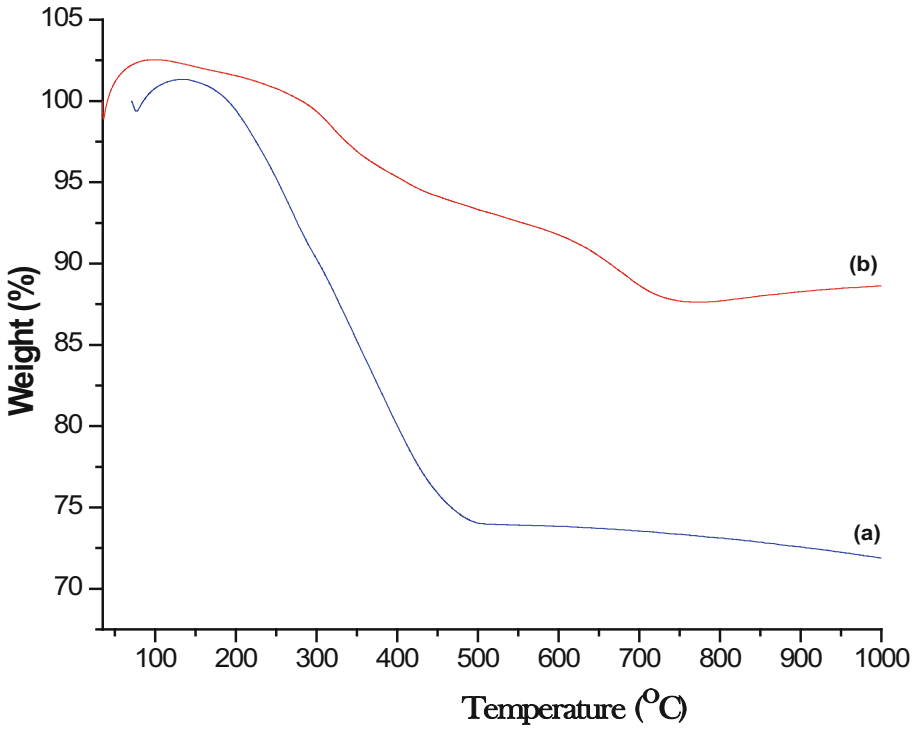

Fig. 5 Thermogravimetric curves of NZFO MNPs. a Bare and b OA–PP123 coated

due to the generation of foam (combustion synthesis using glycine–nitrate mixture results in very high voluminous and foamy powder more so, when more than stoichiometric amount of glycine was used in the synthesis of NZFO MNPs) and contact with furnace wall (Widmann 2001). The weight loss (∼ 28%) in the temperature range of 180–500 °C which is not seen in the coated sample (Fig. 5b) might be due to the complete decomposition of carbonaceous matter resulting from the decomposition of excess glycine fuel (decomposition is consistent with the TGA of glycine). The procedure used for the coating of the bare MNPs with OA–PP123 which involved several washings in organic solvent and water coupled with the heating carried out might have removed the excess glycine seen in the bare sample. It can also be seen that in the 500–1000 °C temperature range, no weight loss is

observed confirming the presence of pure NZFO phase. Therefore, the TG curve suggests that a pure NZFO phase is present since there is no further weight loss seen in the TG curve. For the OA–PP123-coated NZFO sample, two major weight loss processes (consistent with the attached molecules) are observed in the TG curve (Fig. 5b). Similarly, two stage weight loss processes were observed in the TG of OA–Pluronic F127-coated LSMO MNPs (Thorat et al. 2014). The first weight loss ($\sim$ 5%) in the temperature range of 300–450 °C is due to the decomposition of the attached PP123 co-polymer layer from the surface. The second weight loss ($\sim$ 8%) in the temperature range of 450–750 °C is due to the decomposition of the covalently bonded OA molecules to the MNPs' surfaces. Similarly, OA molecules decomposed in the temperature range of 450–600 °C in the TG analysis of OA-capped perovskite lead titanate (Wang et al. 2010). Thus, the TGA study suggests the OA–PP123 coating on the surface of NZFO MNPs.

3.6 Magnetic Properties

The hysteresis loops measured at room temperature for the bare and OA–PP123-coated NZFO MNPs are shown in Fig. 6. The saturation magnetization (M_s), remanent magnetization (M_r), coercivity (H_c) and squareness loop (M_r/M_s) of the bare and coated sample are summarized in Table 2. It can be seen that these values are higher in the coated sample compared to the bare sample. The M_s value of the coated sample (35 emu/g) is higher than the bare sample (32 emu/g) at an applied field of ± 20,000 G at 300 K. Higher M_s values have also been reported for poly vinyl alcohol (PVA)-coated $Ni_{0.3}Zn_{0.7}Fe_2O_4$ MNPs

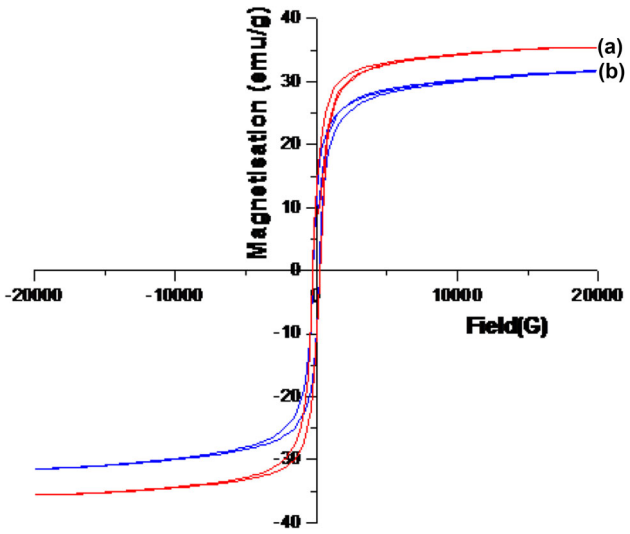

Fig. 6 Magnetic hysteresis curves of NZFO MNPs measured at room temperature for a bare and b OA–PP123 coated

(Rahimi et al. 2013) and Gd-substituted NiCa ferrite/PVA nanocomposite (Prasad and Dolia 2012) systems. The increase in magnetization of the coated sample is probably due to the nanoparticles' crystal growth after polymer coating and spin injection or anti-spin canting being transpired at the surfaces of the MNPs due to the interaction with polymer chain (Prasad and Dolia 2012). Depending on the applications, certain properties of MNP are desired. In most biomedical applications, nanoparticles with higher saturation magnetization are preferred because they provide higher sensitivity and efficiency (Colombo et al. 2012). The coated sample had a higher M_r, H_c and M_r/M_s values than the bare sample. M_s and H_c are important magnetic properties critical to biomedical applications. The tuning of M_s to higher values is very important in biosensing and drug delivery applications (Koh and Josephson 2009; Gazeau et al. 2008) while increased H_c is very important in hyperthermia (Kolhatkar et al. 2013). The results show that OA–PP123 coatings tuned the magnetic properties of M_s and H_c for increased efficiency in biomedical applications.

3.7 Colloidal Stability Study

The colloidal stability of the bare and OA–PP123-coated NZFO sample was evaluated by the zeta potential measurements. Zeta potential measurement is an important parameter for evaluation of MNPs in biomedical applications at physiological pH. The zeta potential distribution of bare and coated sample using distilled water as a dispersant was 11.9 and − 10.35 mV, respectively. The results show there was a flip of charge after OA–PP123 coating. This might be as a result of the ionization of the hydroxyl end of the poly (ethylene oxide) chain when dispersed in water conferring a negative charge on the oxygen atom hence, leading to a negative zeta potential value. The pH-dependent zeta potentials of the coated sample is − 26.2 mV at pH 7.4 (physiological pH) and − 5.86 mV at pH 5.0 (cancer cell endosomal pH). These pH dependent zeta potential values of the OA–PP123-coated sample can be explained by recalling that the negative charge comes from the ionization of the hydroxyl groups. At pH 7.4, more number of the hydroxyl end groups would be ionized making it more negatively charged. At pH 5.0, the hydroxyl ionization is lesser thus lowering the net negative charge. The zeta potential value (− 26.2 mV) of the coated sample at physiological pH implies that the OA–PP123/NZFO composites could maintain their dispersion stability in physiological environment and thus have great potential to be used in hyperthermia as a heating mediator and as a drug delivery vehicle. However, further experiments like hemocompatibility assay, cytotoxicity tests and magnetic

Table 2 Magnetic properties of the bare and the OA–PP123-coated NZFO MNPs

Sample	Saturation magnetisation, M_s (emu/g)	Remanence magnetisation, M_r (emu/g)	Coercivity, H_c (G)	M_r/M_s
Uncoated sample	32	19	224	0.59
OA–PP123	35	24	249	0.69

hyperthermia measurements have to be carried out to test their real therapeutic potentials.

4 Conclusion

This work typically focussed on the effect of OA–PP123 coating on the magneto-structural and colloidal stability study of NZFO MNPs with their potential biomedical applications in mind. The spinel NZFO MNPs have been successfully prepared by the low temperature auto-combustion method using a glycine fuel-rich composition without any further heat treatment at high temperature. The surfaces of the synthesised MNPs were functionalised with OA–PP123 thereby conferring suitable chemical, physical and physiological properties for biomedical applications. XRD results showed the formation of cubic spinel crystalline phase with and without coating of OA–PP123. The results of thermal and spectro-analysis indicated that there was an interaction between OA–PP123 coatings and NZFO MNPs. FE-SEM result shows that there was enlargement of particle size after coating but revealed a more regular shape and lesser agglomeration. After coating, the MNPs retained the hysteresis loop of the ferrimagnetic nature at room temperature under applied magnetic field. The values of M_s and H_c increased with OA–PP123 coatings in the composite. The high zeta potential value of the coated sample at physiological pH is an important parameter for successful application of the nanofluid biomedically. The combination of magnetic properties and the stability of the particles in physiological suspensions suggest that these materials have potentials to be used in biomedical applications. Also, appreciable amount of drug can be loaded on to the polymer shell serving as a drug delivery system.

Acknowledgements This work would not have been possible without the visiting research grant given to Dr. Ehi-Eromosele C.O. by the International Centre for Materials Science, Jawaharlal Nehru Centre for Advanced Scientific Research, Bangalore, India.

References

Apostolov AT, Apostolova IN, Wesselinova JM (2013) Ferrimagnetic nanoparticles for self-controlled magnetic hyperthermia. Eur Phys J B 86:483

Baldi G, Lorenzi G, Ravagli C (2009) Hyperthermic effect of magnetic nanoparticles under electromagnetic field. Process Appl Ceram 3(1–2):103–109

Banerjee SS, Chen DH (2007) Magnetic nanoparticles grafted with cyclodextrin for hydrophobic drug delivery. Chem Mater 19:6345–6349

Chiappetta DA, Sosnik A (2007) Poly (ethylene oxide)-poly (propylene oxide) block copolymer micelles as drug delivery agents. Eur J Pharm Biopharm 66:303–317

Colombo M, Carregal-Romero S, Casula MF, Gutierez L, Morales MP, Bohm IB, Heverhagen JT, Prosperi D, Parak WJ (2012) Biological applications of magnetic nanoparticles. Chem Soc Rev 41:4306–4334

Dorniani D, Kura AU, Hussein-Al-Ali SH, Bin Hussein MZ, Fakurazi S, Shaari AH, Ahmad Z (2014) In vitro sustained release study of gallic acid coated with magnetite-PEG and magnetite-PVA for drug delivery system. Sci World J 2014:1–11. https://doi.org/10.1155/2014/416354 **(Article ID 416354)**

Dutz S, Andra W, Hergt R, Muller R, Oestreich C, Schmidt C, Topfer J, Zeisberger M, Bellemann ME (2007) Influence of dextran coating on the magnetic behaviour of iron oxide nanoparticles. J Magn Magn Mater 311:51–54

Ehi-Eromosele CO, Ita BI, Iweala EEJ, Adalikwu SA, Anawe PAL (2015) Magneto-structural properties of Ni–Zn nanoferrites synthesized by the low-temperature auto-combustion method. Bull Mater Sci 38(5):1465–1472

Gazeau F, Levy M, Wilhelm C (2008) Optimizing magnetic nanoparticle design for nanothermotherapy. Nanomedicine 3:831–844

Gonzales M, Krishnan KM (2007) Phase transfer of highly monodisperse iron oxide nanocrystals with Pluronic F127 for biomedical applications. J Magn Magn Mater 311:59–62

Gul IH, Ahmed W, Maqsood A (2008) Electrical and magnetic characterization of nanocrystalline Ni–Zn ferrite synthesis by co-precipitation route. J Magn Magn Mater 320:270–275

Jadhav SV, Nikam DS, Khot VM, Mali SS, Hong CK, Pawar SH (2015) PVA and PEG functionalised LSMO nanoparticles for magnetic fluid hyperthermia application. Mater Charact 102:209–220

Jordan A, Scholz R, Wust P, Fähling H, Felix R (1999) Magnetic fluid hyperthermia (MFH): cancer treatment with AC magnetic field induced excitation of biocompatible superparamagnetic nanoparticles. J Magn Magn Mater 201:413–419

Kareem SH, Ati AA, Shamsuddin M, Lee SL (2015) Nanostructural, morphological and magnetic studies of PEG/$Mn_{(1-x)}Zn_{(x)}Fe_2O_4$ nanoparticles synthesized by co-precipitation. Ceram Int 41:11702–11709

Kashevsky BE, Kashevsky SB, Korenkov VS, Istomin YP, Terpinskaya TI, Ulashchik VS (2015) Magnetic hyperthermia with hard-magnetic nanoparticles. J Magn Magn Mater 380:335–340

Khairy M (2014) Synthesis, characterization, magnetic and electrical properties of polyaniline/$NiFe_2O_4$ nanocomposite. Synth Metals 189:34–41

Koh I, Josephson L (2009) Magnetic nanoparticle sensors. Sensors 9:8130–8145

Kolhatkar AG, Jamison AC, Litvinov D, Willson RC, Lee RT (2013) Tuning the magnetic properties of nanoparticles. Int J Mol Sci 14:15977–16009

Kulshrestha P, Gogo M, Bahadur D, Banerjee R (2012) In vitro application of paclitaxel loaded magnetoliposomes for combined chemotherapy and hyperthermia. Colloids Surf B 96:1–7

Kuznetsov AA, Shlyakhtin OA, Brusentsov NA, Kuznetsov OA (2002) Smart mediators for self-controlled inductive heating. Eur Cell Mater 3(Suppl. 2):75–77

Mahdavi M, Namvar F, Ahmad MB, Mohamad R (2013) Green biosynthesis and characterization of magnetic iron oxide (Fe_3O_4) nanoparticles using seaweed (*Sargassum muticum*) aqueous extract. Molecules 18:5954–5964

Maier-Hauff K, Uldrich F, Nestler D, Niehoff H, Wust P, Thiesen B, Orawa H, Budach V, Jordan A (2011) Efficacy and safety of intratumoral thermotherapy using magnetic iron-oxide nanoparticles combined with external beam radiotherapy on patients with recurrent glioblastoma multiforme. J Neuro-Oncol 103:317–324

Mamani JB, Costa-Filho AJ, Cornejo DR, Vieirad ED, Gamarra LF (2013) Synthesis and characterization of magnetite nanoparticles coated with lauric acid. Mater Charact 81:28–36

Montagne F, Monval MO, Pichot C, Mozzanega H, Elaissari A (2002) Preparation and characterization of narrow sized (O/W) magnetic emulsion. J Magn Magn Mater 250:302–312

Morales MA, Jain TK, Labhasetwar V, Leslie-Pelecky DL (2005) Magnetic studies of iron oxide nanoparticles coated with oleic acid and Pluronic® block copolymer. J Appl Phys 97:10Q905

Morrison SA, Cahill CL, Carpenter EE, Calvin S, Swaminathan R, McHenry ME, Harris VG (2004) Magnetic and structural properties of nickel zinc ferrite nanoparticles synthesized at room temperature. J Appl Phys 95(11):6392–6395

Nguyen DT, Kyo-Seon K (2014) Functionalization of magnetic nanoparticles for biomedical applications. Korean J Chem Eng 31(8):1289–1305

Prasad AS, Dolia SN (2012) Gd substituted NiCa ferrite/polyvinyl alcohol nanocomposite. J Magn Magn Mater 324:869–872

Rahimi M, Wadajkar A, Subramanian K, Yousef M, Cui WN, Hsieh JT, Nguyen KT (2010) In vitro evaluation of novel polymer-coated magnetic nanoparticles for controlled drug delivery. Nanomed Nanotechnol Biol Med 6:672–680

Rahimi M, Kameli P, Ranjbar M, Salamati H (2013) The Effect of polyvinyl alcohol (PVA) coating on structural, magnetic properties and spin dynamics of $Ni_{0.3}Zn_{0.7}Fe_2O_4$ ferrite nanoparticles. J Magn Magn Mater 347:139–145

Sakellari D, Brintakis K, Kostopoulou A, Myrovali E, Simeonidis K, Lappas A, Angelakeris M (2016) Ferrimagnetic nanocrystal assemblies as versatile magnetic particle hyperthermia mediators. Mater Sci Eng C 58:187–193

Shah SA, Asdi MH, Hashmi MU, Umar MF, Awan S (2012) Thermoresponsive copolymer coated $MnFe_2O_4$ magnetic nanoparticles for hyperthermia therapy and controlled drug delivery. Mater Chem Phys 137:365–371

Song H, He R, Wang K, Ruan J, Bao C, Li N, Ji J, Cui D (2009) Anti-HIF-1α antibody-conjugated pluronic triblock copolymers Encapsulated with Paclitaxel for tumor targeting therapy. Biomaterials 30(36):6955–6963

Thorat ND, Otari SV, Bohara RA, Yadav HM, Khot VM, Salunkhe AB, Phdatre MR, Prasad AI, Ningthoujam RS, Pawar SH (2014) Structured superparamagnetic nanoparticles for high performance mediator of magnetic fluid hyperthermia: synthesis, colloidal stability and biocompatibility evaluation. Mater Sci Eng C 42:637–646

Uskokovic V, Kosak A, Drofenik M (2006) Preparation of silica-coated lanthanum strontium manganite particles with designable curie point for application in hyperthermia treatments. Int J Appl Ceram Technol 3(2):134–143

Wang J, Pang X, Akinc M, Lin Z (2010) Synthesis and characterization of perovskite $PbTiO_3$ nanoparticles with solution processability. J Mater Chem 20:5945–5949

Widmann G (2001) Interpreting TGA curves. In: Information for users of Mettler Toledo thermal analysis systems. UserCom 1, Switzerland, p 1